

ELECTRONIC AND MAGNETIC PROPERTIES OF Fe₂N and FeN: TRENDS OF THE MAGNETISM OF THE Fe–N SYSTEM*

S. MATAR

L.C.S.-C.N.R.S., Université Bordeaux 1, F-33405 Talence, France

P. MOHN

Technical University of Vienna, A-1060 Vienna, Austria

(Received September 9, 1992; in final form October 26, 1992)

The electronic and magnetic properties of the nitrides Fe₂N and hypothetical FeN were investigated by use of the ASW method. For both nitrides, the calculations were done in the orthorhombic structure of Fe₂N for the two nitrides. The magnetization is low (0.95 μB/at.) for Fe₂N and vanishes for FeN. The decrease of the magnetization with increasing amount of N is assessed within the Fe–N system in a model derived from a Slater-Pauling type behavior. Accordingly, a trend from weak to strong ferromagnetism is suggested.

1. INTRODUCTION

The iron-nitrogen system has been largely investigated since the beginning of the century [1] involving several fields of interest in magnetism (magnetic recording [2], thin layers [3], etc. . .). More recently, band structure calculations aimed to understand the role of nitrogen on the magnetic properties of nitrides were performed for Fe₄N, Fe₈N and Fe₃N using the ASW (augmented spherical wave) method [4,5,6] and by the LMTO method [7]. A general agreement between the calculated results and with experiment was found.

The purpose of this work is to complete the *ab initio* studies of the electronic and magnetic structures of iron nitrides by the calculation of the properties of Fe₂N and hypothetical FeN and to establish trends in the magnetic behavior of the Fe–N system.

2. SETUP OF THE STRUCTURE OF Fe₂N AND FeN

Within the Fe–N system the occurrence of an orthorhombic δ-iron nitride can be understood starting from the hexagonal ε-phase [1]. Along the c axis the ε-structure

* This article is dedicated to Professor J.B. Goodenough (University of Austin-Texas, USA) on his 70th birthday.

can be considered as a succession of A–B–A–B, i.e. Fe–(N)–Fe–(N) layers with N acting as a *spacer* in the Fe lattice. Vacant sites alternate with N in the B layers so that short N–N distances along c are avoided. However, this occurs when the nitrogen content is increased until half of the vacancies are occupied. At such a composition, 2 nitrogen atoms along c are at a distance of $c/2$, too short to allow for the hexagonal arrangement of the atoms to be preserved. Consequently, a transformation to an orthorhombic symmetry occurs for a composition corresponding to Fe_2N .

Fig. 1 shows a projection of the structure with the crystallographic positions of iron and nitrogen. In the Fe_2N structure, the a' , b' , c' and d' nitrogen positions are vacant, being above and below the occupied positions. For the band structure calculations, empty spheres (ES), i.e., pseudo atoms with $Z = 0$ were placed at these positions. These ES prevent too large an overlap between the atomic spheres in the ASA (atomic sphere approximation) and allow for a smooth variation of the potential in the interatomic region.

To our knowledge, Fe_2N corresponds to the highest amount of nitrogen in the Fe–N system. However, for the purposes of the analysis of the magnetic trends within this system, we have simulated the hypothetical 1:1 composition, i.e., FeN within the structure of Fe_2N by adding extra nitrogen atoms (at the positions of the ES in Fe_2N) in the manner shown in *Fig. 1*.

3. ASW CALCULATIONS AND RESULTS

As in the former studies, the ASW method [8] was used to calculate the electronic and magnetic structures of the two nitrides. The calculations are based on the local spin density functional theory in which exchange and correlation effects are treated within the scheme of von Barth and Hedin [9] and Janak [10]. The Brillouin-zone integration is carried out for a sufficiently large number of k points in the irreducible wedge of the first zone of the simple orthorhombic lattice in order to obtain reliable values, i.e., until no further variation occurs, of magnetic moments and total energies of the systems. In this work, 64 k points were used. The matrix elements were constructed using partial waves up to $l_{max} + 1$ ($l_{max} = 2$ for Fe and $l_{max} = 1$ for N). The $l + 1$ components are used for the internal summations in the three-center terms of the matrix elements. Spin-polarized calculations, i.e., for magnetic order, were done in the two structures. One additional non-spin-polarized calculation was done for Fe_2N . The ASW method uses the ASA where each atom is surrounded by a sphere wherein the potential and the charge density are assumed to be spherically symmetric. The space outside the spheres is not accounted for but the sum of the volumes of all the spheres is equal to the volume of the unit cell. The various sphere radii are chosen to give the minimum total energy for given cell volume.

3.1 Charge Distribution

Fe_2N . The obtained partial charges at each lattice site in Fe_2N are given in *table 1a* for the spin-polarized (SP) calculation, i.e., spin-projected charges along ma-

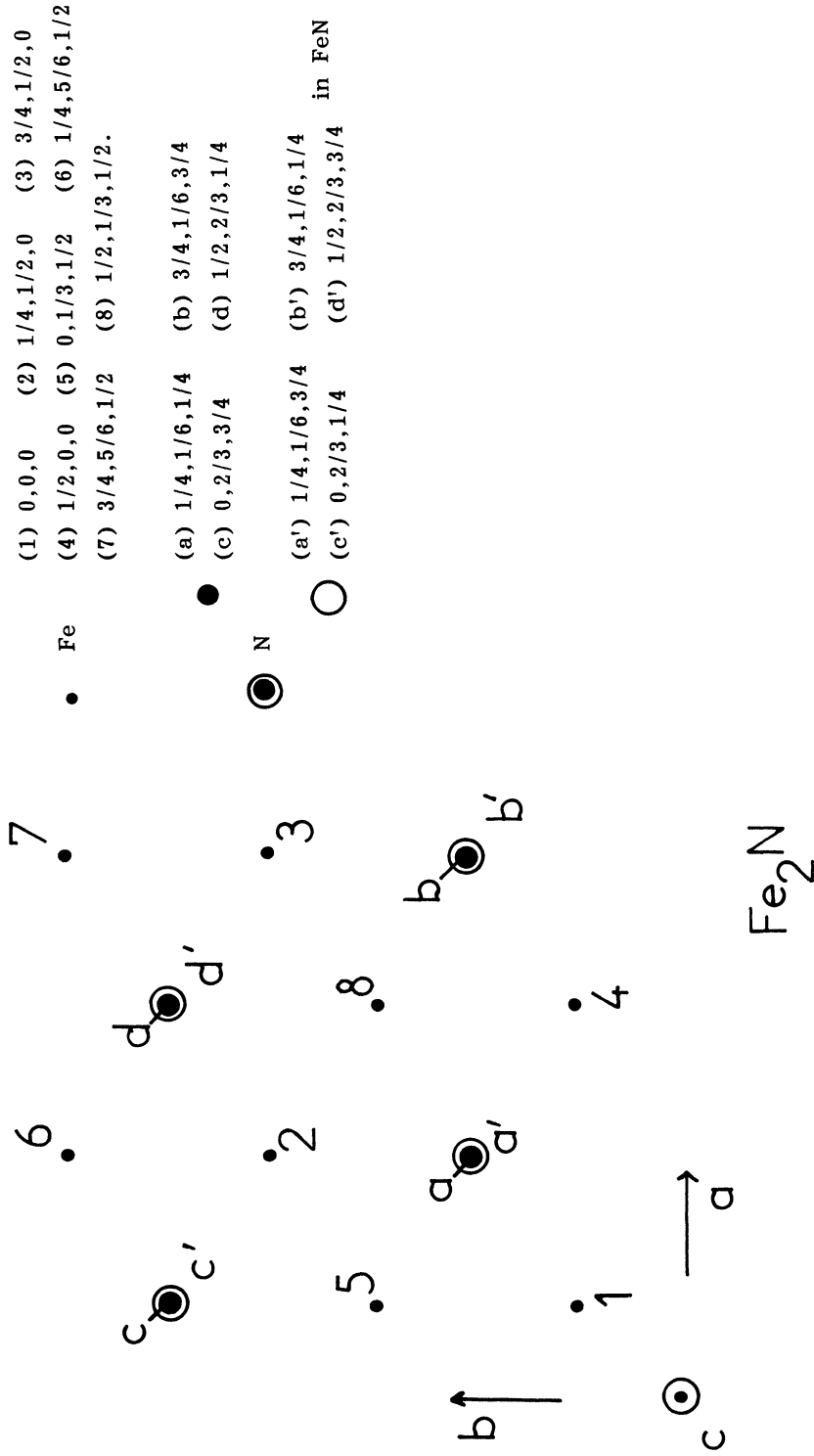


FIGURE 1 Projection of the orthorhombic Fe_2N structure showing the respective positions of Fe and N (black spheres). N open sphere positions are occupied in hypothetical FeN.

TABLE 1
Local partial charges for Fe₂N.

$a = 10.39696$ a.u.₃; $b/a = 0.87453$; $c/a = 0.80364$.

$V = 789.874$ a.u. $Z = 4$ f.u.

$r_{ws}(Fe) = 2.66168$ a.u.; $r_{ws}(N,ES) = 1.67675$ a.u.

a) spin polarized (S.P.) calculations.

64k	$n_s \uparrow$	$n_s \downarrow$	$n_p \uparrow$	$n_p \downarrow$	$n_d \uparrow$	$n_d \downarrow$	$n_f \uparrow$	$n_f \downarrow$	$M_{\mu B}$	Q_{TOT}
Fe	0.26	0.26	0.42	0.42	4.10	2.61	0.08	0.08	1.47	8.23
N	0.62	0.62	1.38	1.45	0.02	0.02	—	—	-0.07	4.11
ES	0.12	0.14	0.07	0.07	—	—	—	—	-0.01	0.4

$E_F = 0.85816$ Ryd. $Q(\text{Valence}) = 84$

$E(\text{Variational})/f.u. = -5190.74083$ Ryd.

b) non spin polarized (NSP) calculations.

64k	s	p	d	f	Q
Fe	0.52	0.83	6.74	0.17	8.26
N	1.23	2.82	0.04	—	4.09
ES	0.26	0.13	—	—	0.39

$E_F = 0.84221$ Ryd. $Q(\text{Valence}) = 84$

$E(\text{Variational})/f.u. = -5190.722587$ Ryd.

$\Delta E_{var}(\text{SP} - \text{NSP}) = -0.0182425$ Ryd./f.u.

majority (\uparrow) and minority (\downarrow) spin directions and in *table 1b* for the non-spin-polarized (NSP) calculation. A small charge transfer occurs from nitrogen to iron and the ES. The bonding in this system can be considered as covalent. The count of the s and p partial charges for either one of the spin directions for Fe is equal to 0.68. This value is close to the electron count of 0.65 for $sp(\uparrow)$ found in our recent calculations on Fe₃N [6] and will be further discussed below.

From *table 1b* showing the ASW results of non-spin-polarized ASW calculations on Fe₂N, the respective local partial charges are close to the sums of spin-projected charges in *table 1a*. A net stabilization of the spin polarized state by -0.01287 Ryd. (-0.175 eV) per formula unit (f.u.) is observed. This points to a stable ferromagnetic state for this nitride.

FeN. *Table 2* shows the site and spin projected partial charges for spin-polarized calculations of FeN. For this nitride too, there is a small charge transfer from nitrogen to iron. The electron count of s and p electrons for either spin directions of 0.65 is close to the value found for Fe₂N. This nearly constant value seems to characterize the three nitrides Fe₃N, Fe₂N and FeN and will be addressed in section 4.

3.2 Magnetic Moments

From *table 1a* it is mainly the $3d$ intra-band polarization which provides the moment for Fe. Its magnitude for Fe₂N ($1.47 \mu B$) is lower than that calculated for Fe₃N ($2.15 \mu B$). The unbalance in the $2p$ states of nitrogen between majority (\uparrow) and minority (\downarrow) spins is in favor of the latter leading to the negative value of the

TABLE 2
Local partial charges for FeN.

$a = 10.39696$ a.u.; $b/a = 0.87453$; $c/a = 0.80364$.
 $V = 789.874$ a.u. $Z = 4$ f.u.
 $r_{ws}(Fe) = 2.50127$ a.u.; $r_{ws}(N,ES) = 1.98526$ a.u.

64k	$n_s \uparrow$	$n_s \downarrow$	$n_p \uparrow$	$n_p \downarrow$	$n_d \uparrow$	$n_d \downarrow$	$n_f \uparrow$	$n_f \downarrow$	$M_{\mu B}$	Q_{TOR}
Fe	0.24	0.24	0.41	0.41	3.31	3.31	0.10	0.10	0.0	8.11
N	0.73	0.73	1.65	1.65	0.06	0.06	—	—	0.0	4.88

$E_F = 1.03351$ Ryd. $Q(\text{Valence}) = 104$
 $E(\text{Variational})/f.u. = -2649.7819$ Ryd.

moment. The average moment per atom in Fe_2N is close to $0.95 \mu_B$. No experimental data from the literature are available for the magnetic moment of Fe in Fe_2N . Although Bridelle's investigations [11] give a low magnetization, Mössbauer studies by Bainbridge *et al.* [12] are in favor of the absence of magnetic order.

For FeN, the absence of polarization for the Fe- $3d$ states leads to a zero moment and to a balance in electron occupation for N s and p states. Thus FeN is found to be non-magnetic.

3.3 Densities of States (DOS)

The total spin-projected DOS are shown for Fe_2N and FeN in *figs. 2 & 3* respectively. They are representative of the two sets of calculations of *tables 1a & 2*. Energies are counted with respect to E_F at 0.8582 and 1.0335 Ryd. for the two nitrides respectively.

From left to right the DOS present the following features: N($2s$), N($2p$) and Fe($3d$) states crossed by E_F . The spectral weights for the two spin directions are nearly equal in the two nitrides, contrary to those for Fe_8N and Fe_4N . This points to a magnetization induced by a rigid band shift, at least for Fe_2N , which could be described within a Stoner model, whereas the DOS of Fe_8N and Fe_4N had to be described on the basis of a non-rigid shift within a "covalent magnetism" model [13]. The main difference between the DOS of Fe_2N and FeN lies in the broadness of the latter ones, i.e., a strong hybridization between the states of N($2s$, $2p$) and Fe($3d$), which are closer in energy than those of Fe_2N (see the energy position of the respective N($2s$) states).

E_F crosses the total DOS at Fe($3d$) states. This occurs for Fe_2N at a minimum for majority spins and a maximum for minority spins. This feature, already observed for similar calculations on T_3X (T: transition metal, X: non-metal) compounds by Malozemoff *et al.* [14], led us to plot the site and l projected DOS for Fe. This is shown in *Fig. 4*. Fe(s) and Fe(p) DOS are at a minimum at E_F for the latter two DOS indicating a "hybridization gap" [14], which helps to hold the sp (\uparrow) population constant and leads to a strongly ferromagnetic behavior (see section 4). On the contrary, for FeN, which is non-magnetic, E_F crosses the Fe($3d$) states at a maximum of DOS just above a minimum. This feature is similar for the calculation of non-spin polarized Fe_2N in *fig. 4*. For both nitrides the large DOS at E_F is

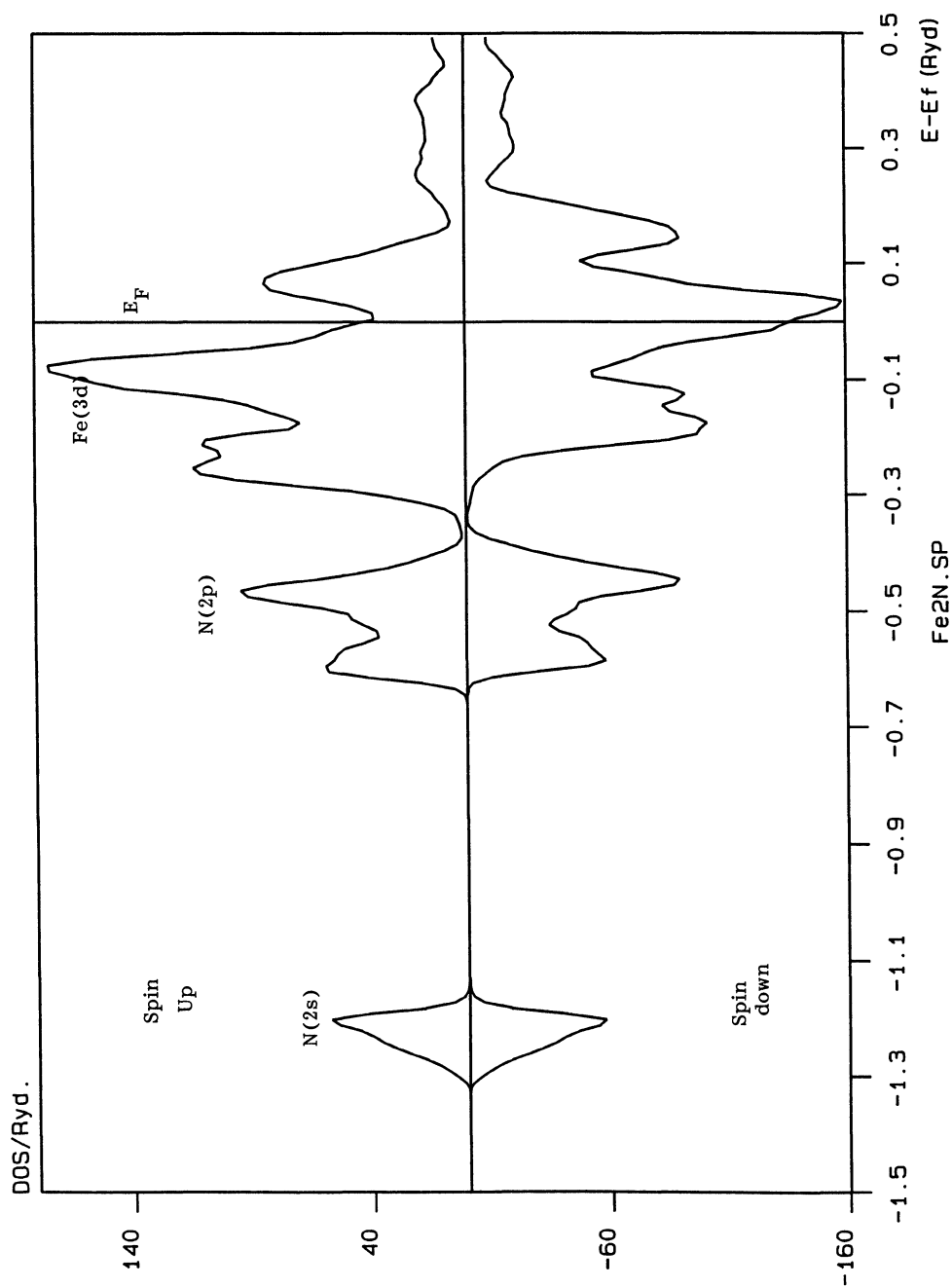


FIGURE 2 Total spin projected densities of states of Fe₃N. Energies are counted with respect to E_F at 0.8582 Rydbergs.

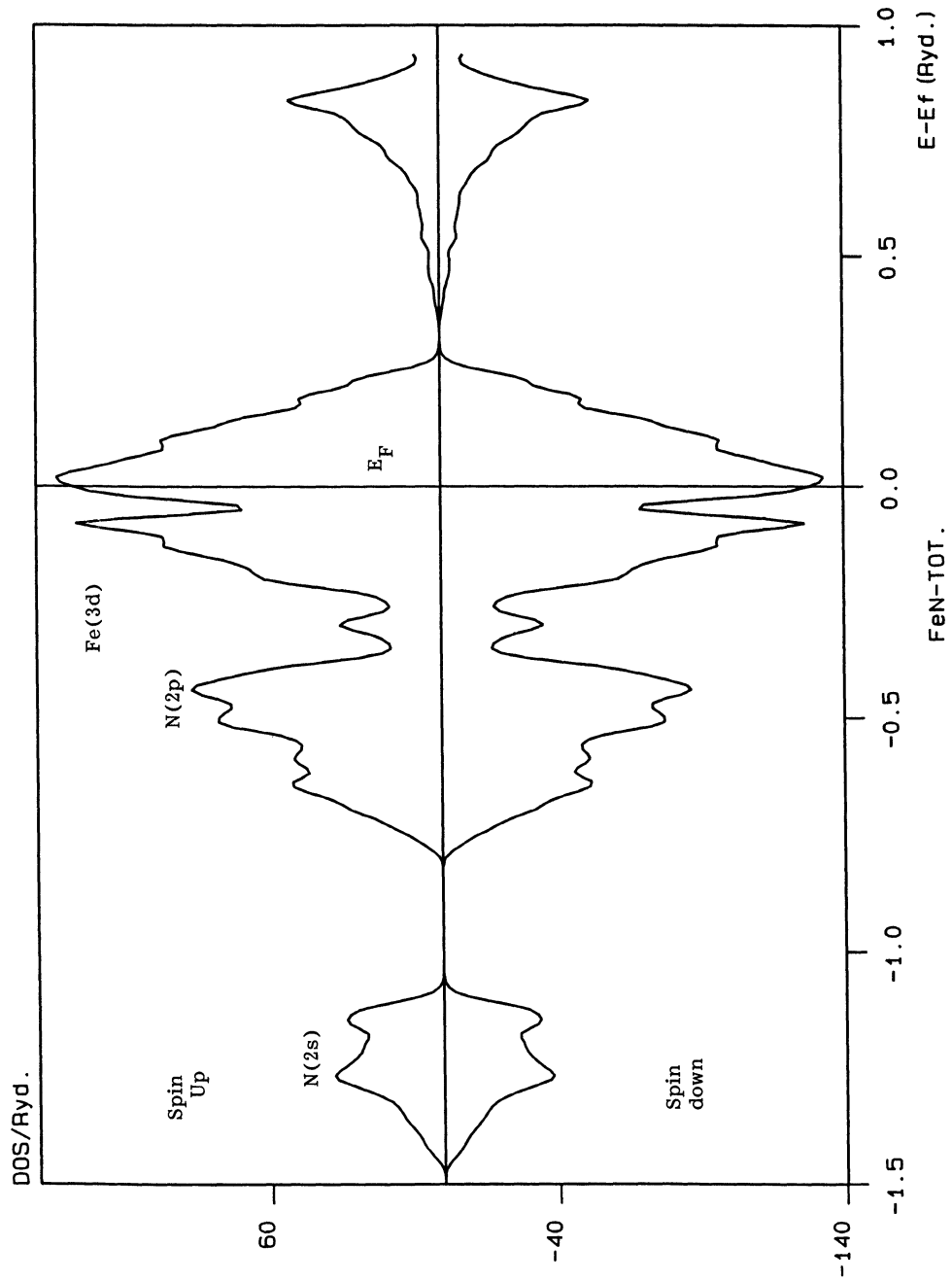
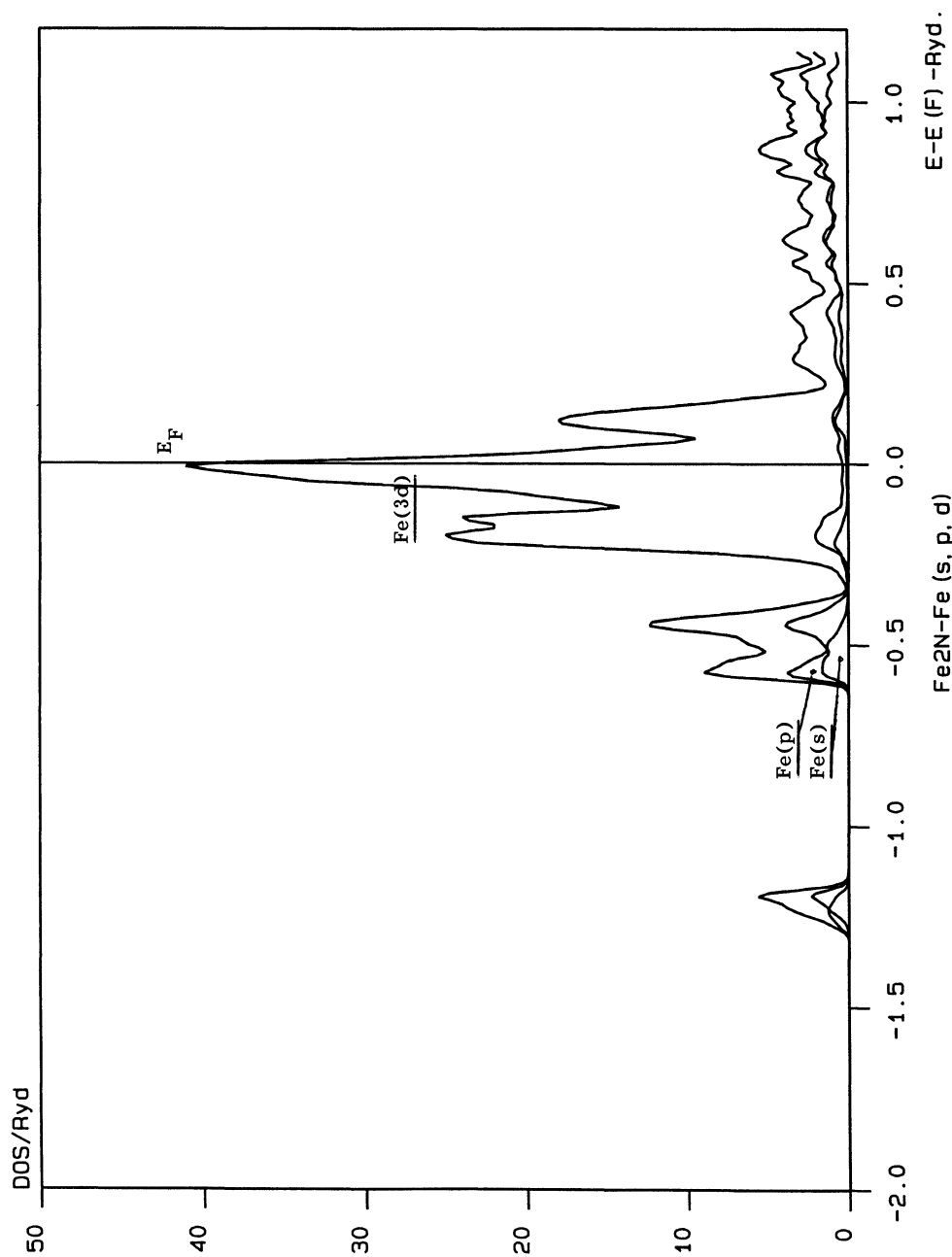


FIGURE 3 Total spin projected densities of states of FeN. Energies are counted with respect to E_F at 1.0335 Rydbergs.

FIGURE 4 *I*-projected densities of states of Fe for non-spin polarized Fe₂N.

indicative of a metallic type behavior, and they can be considered as itinerant ferromagnets.

For a more detailed description of the DOS of iron nitrides, the reader is referred to References 4, 5, 6.

4. THE SLATER-PAULING CURVE

In this section we discuss the variation of the magnetization in the two presently studied nitrides and within the Fe-N system as a whole, by means of a model based on the Slater-Pauling curve.

The Slater-Pauling curve is a plot of the average magnetic moment μ_{av} with the valence electron count Z_v for intermetallic alloy systems characterized by strong ferromagnetism. It accounts for the variation of the average magnetization of an alloy with solute concentration.

For most of the magnetic systems, either the majority ($n \uparrow$) or minority ($n \downarrow$) spin count is known. The magnetization being provided by the difference of electron occupation between majority (\uparrow) and minority (\downarrow) spins and the system being neutral, the following relationships can be established:

$$m = n \uparrow - n \downarrow \text{ and } Z_v = n \uparrow + n \downarrow .$$

Hence m can be obtained either as:

$$m = 2n \uparrow - Z_v \quad - \text{ if } n \uparrow \text{ is known,} \quad (1)$$

or as:

$$m = Z_v - 2n \downarrow \quad - \text{ if } n \downarrow \text{ is known.} \quad (2)$$

(1) and (2) describe two branches with opposite 45° slopes of the SP curve around which the experimental points gather.

As the magnetic moment mostly arises from d-band polarization, the quantity "magnetic valence" can be defined - here for systems where $n_{d\uparrow}$ is known - by the relationship [14]:

$$Z_m = 2n_{d\uparrow} - Z_v \quad (3)$$

Upon alloying, the electron count of the d states changes discretely as stated by Friedel [15], so that $n_{d\uparrow}$ is either 0 (early transition elements) or 5 (late transition elements). For instance, for Fe, Z_v is 8 and $Z_m = 10 - 8 = 2$, whereas for N, $n_{d\uparrow} = 0$ when $Z_v = 3$ and $Z_m = 0 - 3 = -3$. This leads to an alternative plot of the SP-curve called the Slater-Pauling-Friedel (SPF) [16] curve where μ_{av} is plotted against Z_m :

$$\mu_{av} = Z_m + 0.6 \quad (4)$$

In (4), 0.6 is a nearly constant contribution to the moment arising from s and p electrons. Referring the reader to [14,16] for a detailed description, we just examine the series of the 3d ferromagnetic elements Fe, Co and Ni. As stated above, for these elements $n_{d\uparrow}$ is 5. Their average moments $\mu_{av.}$ calculated via (4) are given in *table 3*. This yields the correct moments for Co and Ni whereas that of Fe (2.60 μ B) is much larger than the experimental value of 2.22 μ B. In this sense, Co and Ni are strong ferromagnets whereas Fe is a weak ferromagnet. From the point of view of band structure, this means that the majority-spin (\uparrow) densities of states (DOS) of Co and Ni all lie below the Fermi energy (E_F) and any localized perturbation is not likely to modify them, whence the ‘‘strong’’ ferromagnetism, contrary to Fe whose DOS are penetrated by E_F .

4.1 Application to Iron Nitrides

The calculated atom-averaged magnetic moments via (4) and from ASW calculations on one hand and experimental values from literature on the other hand are given in *table 3* for iron nitrides. A general agreement with {ASW} is found with data from recent *ab initio* calculations of nitrides [7]. All average moments decrease with increasing amount of nitrogen in the series and the agreement to a vanishing moment for FeN is well predicted from (4) and ASW calculations. From *table 3* it is interesting to note the constant value of $Z_v - Z_m = 6$. This can be trivially derived for any Fe_xN nitride as follows ($Z = Z(Fe) = 8$ and $Z' = Z(N) = 3$):

$$Z_v - Z_m = \frac{xZ + Z'}{x + 1} - \frac{x(10 - Z) - Z'}{x + 1} = 6 \quad (5)$$

Fig. 5 shows a plot of the calculated and experimental average magnetizations with Z_v or Z_m for the different iron nitrides (cf *table 3*). With a good approximation, the points corresponding to all nitrides lie on two straight lines for the experimental {EXP} and calculated {ASW} data. An additional plot of $\mu_{av.}$ from (4) is shown as well, i.e., line {SPF}. Whereas {ASW} and {SPF} lines are parallel and very close, the slope of the {EXP} lines are parallel and very close, the slope of the {EXP} line is higher. Hence a cross-over can be seen at Fe_3N .

TABLE 3
Magnetic and valence electron counts and magnetic moments for 3d elemental magnets and iron nitrides.

	$Z_{val.}$ at.	$Z_{magn.}$ /at.	$Z_v - Z_m$ /at	$\mu = Z_m + .6$	$\mu_{calc.}$ [18]	$\mu_{exp.}$ [19]
α -Fe	8	2	6	2.60	2.15	2.22
α -Co	9	1	8	1.60	1.70	1.71
γ -Ni	10	0	10	0.60	0.60	0.60
Fe8N	7.44	1.44	6	2.04	[4,5,6] 2.17	[20-22] 2.40
Fe4N	7.0	1.0	6	1.60	1.67	1.80
Fe3N	6.75	0.75	6	1.35	1.44	1.33
Fe2N	6.33	0.33	6	0.93	0.95	—
FeN	5.5	-0.5	6	0.10	0.0	—

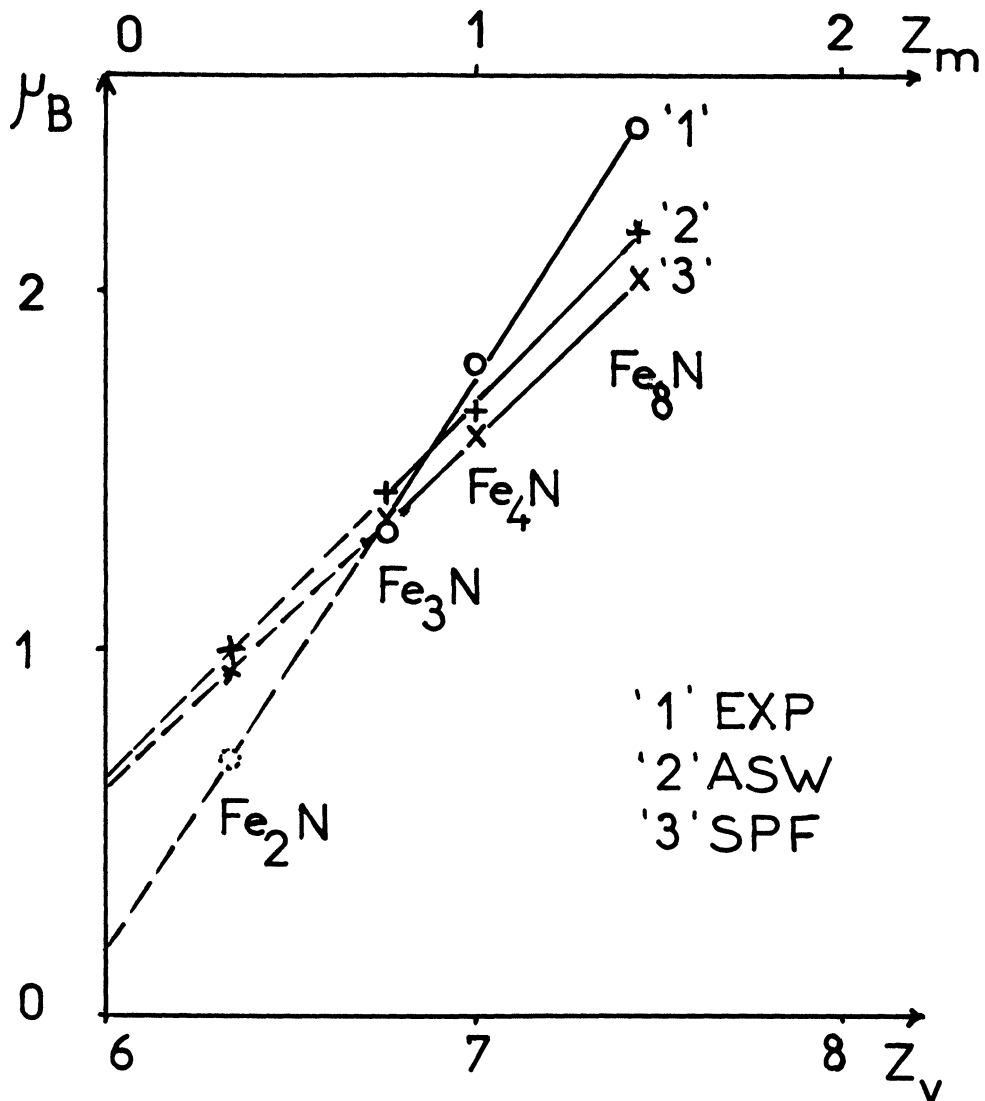


FIGURE 5 Variation of the experimental {EXP} and calculated {ASW} and {SPF} values of average magnetic moment for the series of iron nitrides.

The {ASW} line has a slope very close to the {SPF} line and it is found to obey the following equation:

$$\mu_{av.} = Z_m + 0.65 \quad (6)$$

Whereas the proximity of (6) to (4) suggests that the nitrides, from the point of view of band structure calculations would obey a Slater-Pauling-Friedel like behavior, the "0.65" figure in (6) deserves some attention. This is the electron count

found in the present calculations of Fe_2N and FeN , and in recent ASW calculations for $\text{SP} \uparrow$ in Fe_3N [6]. The result was assessed in connection with similar calculations by Malozemoff *et al.* [14] for a family of T_3X compounds ($\text{T} = \text{Fe}, \text{Co}$; $\text{X} = \text{metal}$ or non-metal solute). Although no data were given for N or another member of its group, it appears that for our nitrides the $\text{sp} \uparrow$ electron count is held constant by the attractive potential of the solute. The theory establishes that the hybridization of the sp states with the d states results in a depression near the Fermi level of the sp DOS of the metal, i.e., states that would respond to the stronger sp potential of the non-metal. This feature, which was observed for Fe_3N [6], can be seen for the DOS of Fe_2N shown in Fig. 4. However, no such feature could be observed for the DOS of FeN .

4.1.1 Magnetic Trends Within the Fe–N System

The cross-over between experimental and calculated lines in Fig. 5 defines two distinct regions for Fe-nitrides: those whose calculated values of magnetizations are below experimental values, i.e., Fe_8N and Fe_4N , and those for which this is reversed, i.e., Fe_3N and Fe_2N . A close agreement between experimental and calculated moments from (1) for Fe_3N (see table 1) can be noticed. The consequence is that the member of the Fe–N system, which strictly obeys an SPF-type behavior is Fe_3N , i.e., it is a strong ferromagnet in the same way as intermetallic alloys [16] and T_3X [14]. Fe_2N would behave similarly. In as far as experimental points are concerned, Fe_8N and Fe_4N would rather behave as weak ferromagnets as their corresponding points lie above the SPF-line.

4.1.2 Volume vs Bonding Effects

The tendency of the calculated {ASW} line to align nearly parallel to the {SPF} line could be a consequence of band-structure calculation versus volume. It has been established [17] that the magnetic moment of Fe and the type of magnetic behavior greatly depends on volume. In the Fe–N system (experimentally) a major role is played by nitrogen in the volume expansion of the Fe lattice. Obviously this effect increases upon increasing amount of N, i.e., going through the series Fe_8N , Fe_4N , Fe_3N , Fe_2N and FeN and should lead to an increase of the moment of Fe.

However, the second role of N is a spin-pairing effect between one spin of N-2p and one spin of Fe-3d. This leads to a loss of one Fe spin. It is probable that for the highest term in the series, i.e., hypothetical FeN , the Fe–Fe exchange coupling would be so much weakened by the surrounding nitrogen shells that all magnetic order is lost.

The discrepancy between the experimental and the calculated lines is most pronounced for the two extreme nitrides; Fe_8N and Fe_2N . For the former, which is prepared by thin film techniques, the giant moment could be a result of large lattice distortions of the α -Fe lattice induced by the insertion of nitrogen (i.e., possible clustering effects that cannot be accounted for by *ab initio* calculations). For Fe_2N , which can be prepared as fine powders, further experimental work is being undertaken in order to give a precise value of the magnetization.

ACKNOWLEDGMENTS

The authors thank Prof. J. Kübler of the Technical University of Darmstadt for fruitful discussions at an early stage of this work.

REFERENCES

1. Jack K.H., Proc. Roy. Soc. of London, *A1*, 34 (1948).
2. Tasaki A., Harada S. and Kusunose T., Proc. of Int. Conf. on Ferrites (Japan), 208 (1980).
3. Kim T.K., Takahashi M., Appl. Phys. Lett. *20*, 492 (1972).
4. Matar S., Mohn P., Demazeau G. and Siberchicot B., J. Phys *France*, *49*, 1761 (1988).
5. Matar S., Z. Physik B, Cond. Matt., *87*, 91 (1992).
6. Matar S., Siberchicot B, Pénicau M. and Demazeau G., J. Phys. I, *France*, *2*, 1819 (1992).
7. Sakuma A., J. Magn. & Magn. Mat., *102*, 127 (1991).
8. Williams A.R., Kübler J. and Gelatt C.D. Jr, Phys. Rev. *B19*, 6094 (1979).
9. von Barth J. and Hedin D., J. Phys. C *5*, 1629 (1972).
10. Janak J.F., Solid State Commun., *25*, 53 (1978).
11. Bridelle R., Ann. de Chim., *t. 10*, 824 (1955).
12. Bainbridge J., Channing D.A., Whitlow W.H. and Pendlebury R.E., J. Phys. Chem. Solids, *34*, 1579 (1973).
13. Williams A.R., Zeller R., Moruzzi V.L., Gelatt C.D. Jr and Kübler J., J. Appl. Phys., *52*, 2067 (1981).
14. Malozemoff A.P., Williams A.R. and Moruzzi V.L., Phys. Rev. *B29*, 1620 (1984).
15. Friedel J., Nuevo Cimento *10*, Suppl. 2, 287 (1958).
16. Kübler J. and Eyert V. in *Electronic and Magnetic Properties of Metals and Ceramics*. Buschow K.H.J. Ed. (VCH Verlagsgesellschaft) 1991.
17. Kübler J., Phys. Lett. *A81*, 81 (1981).
18. Moruzzi V.L., Janak J.F., Williams A.R. in *Calculated Electronic Properties of Metals*. Pergamon Press Inc., New-York (1978).
19. Bozorth R. in *Ferromagnetism*, Wiley & Sons, N.Y. (1951).
20. Kim T.K., Takahashi M., Appl. Phys. Lett. *20*, 492 (1972).
21. Wiener G.W. and Berger J.A., J. Met. *7*, 360 (1955).
22. Robbins M. and White J.G., J. Phys. Chem. Solids, *25*, 717 (1964).



Hindawi

Submit your manuscripts at
<http://www.hindawi.com>

